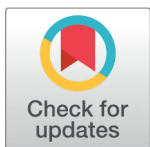


RESEARCH ARTICLE



Thermal Behaviour of Tamarind Seed Kernel Based Bio-Composites Intended for Thermal Insulation

 OPEN ACCESS

Received: 10-01-2022

Accepted: 27-03-2022

Published: 25-05-2022

Kushal G Ambli^{1*}, B M Angadi², Mohan B Vanarotti³¹ Visvesvaraya Technological University, Belagavi, 590018, India² BLDEA's V. P. Dr. P. G. Halakatti College of Engineering and Technology, Vijayapur, India³ Sanjeevan Engineering and Technology Institute, 416201, Panhala, India

Citation: Ambli KG, Angadi BM, Vanarotti MB (2022) Thermal Behaviour of Tamarind Seed Kernel Based Bio-Composites Intended for Thermal Insulation. Indian Journal of Science and Technology 15(19): 927-937. <https://doi.org/10.17485/IJST/v15i19.75>

* **Corresponding author.**

kushalambli@gmail.com

Funding: None

Competing Interests: None

Copyright: © 2022 Ambli et al. This is an open access article distributed under the terms of the [Creative Commons Attribution License](https://creativecommons.org/licenses/by/4.0/), which permits unrestricted use, distribution, and reproduction in any medium, provided the original author and source are credited.

Published By Indian Society for Education and Environment ([iSee](https://www.isee.org/))

ISSN

Print: 0974-6846

Electronic: 0974-5645

Abstract

Objective: Current research is aimed to emphasize the use of bio-based composites in the form of thermal insulation, achieving complete degradability. Low density bio-composites have gained moderate importance as its development is in its primitive stage because of the processing and preparation issues. **Methods:** A preliminary investigation is carried out based on the results of the selected reinforcements Eggshell (ES), Groundnut Pod (GP), and Paper Cellulose (PC) with Tamarind Seed Gum (TSG) binder to justify the thermal behaviour in terms of thermal conductivity, thermal resistivity and diffusivity of various compositions; also conducted morphological characterization to justify molecular level bonding phenomenon. The fungal development on the composites is predominant and is addressed by use of additives, the additive samples are tested and analysed for change in properties. **Findings:** The preliminary experimental results motivated the use of PC reinforcement for further investigation. The samples of various compositions are synthesized for further testing. The average 'k' obtained from ES, GP, and PC based composites is 0.13, 0.083 & 0.052 W/mk respectively. The PC based composites depicted promising results in contrast with the commercially used insulation materials. **Novelty:** Considering the harmful effect of commercially used non-degradable insulation materials, an attempt is made in this research to synthesize a new completely biodegradable composite material for thermal insulation.

Keywords: Morphology; thermal properties; theoretical model; biocomposites; density

1 Introduction

Traditional insulation materials like fiberglass, mineral wool, cellulose, polyurethane foam, Polystyrene etc, are extensively used in buildings. Due to recent developments in the field of thermal insulation, there is enhancement in the desired properties, but these developments do not address the issue of their impact on the environment⁽¹⁾. Some of these materials are non-degradable and possess a certain threat to the environment, impacting it⁽²⁾. It's important to develop new material that possess the required properties without affecting the environment. Feasible solution is to employ

the naturally available or artificially synthesized degradable materials which involve minimal processing and can be manufactured in the form of composites.

As per the requirement, materials can be characterized in to organic and inorganic insulation materials⁽³⁾. Most metals possess high thermal conductivity limiting its use in thermal insulation, this emphasized use of non-metallic's for the said application.

Many researchers have developed composite based materials using natural reinforcements with a combination of synthetic based polymer binders like phenolic, epoxy, polyurethane, and polyester based resins⁽⁴⁾, some of which possess better retardation against fire and better dimensional stability along with better strength but are non-degradable.

The literature study presented the consolidate research carried out by various researchers in the field of thermal insulation⁽⁵⁾, compare the fillers incorporated in composites in terms of thermal conductivity, and correlate thermal conductivity with the density. The present article deals with the performance of the synthesized composites in terms of composite thermal insulation to minimize heat loss maintaining the required temperature inside the building.

By the extensive literature review, tamarind seed gum is considered as the binder for present application. Tamarind seed powder is obtained from the kernel (Seed core) gathered from tamarind tree (*Tamarindus indica*) is a by-product of tamarind pulp. Kernel powder in a wet state is a creamy white to light tan in colour. A small amount of fat is present in the seed causing a tendency for the gum to form lumps.

Table 1. Composition of tamarind seed kernel⁽⁶⁾.

| Content | Percentage |
|-------------------------|----------------|
| Protein | 15.4% to 22.7% |
| Oil | 3.0% to 7.4% |
| Crude fiber | 7% to 8.2% |
| Non-fiber carbohydrates | 61% to 72.2% |
| Ash | 2.45% to 3.3% |

The composition (Table 1) of seed kernel determines the bonding characteristics of the synthesized composite. The kernel powder is dispersible in the water when gum starts to form in the form of gel giving a smooth, continuous, and elastic film, possesses moisture content of 11.3 ± 1.4 %. The bulk density of tamarind seed is marginally higher for the whole raw seed (821 to 840 kgm^{-3}) than for the roasted kernel (760 to 771 kgm^{-3}). The roasted tamarind kernel can absorb water at 245.7 ± 6.2 and $196.6 \pm 5.0 \text{ gms/hr}$.

Table 2. The mineral content of tamarind seed kernel

| Mineral Content | Quantity |
|-----------------|-----------------|
| Calcium | 120.0 mg/100 g |
| Magnesium | 180.0 mg/100 g |
| Potassium | 1020.0 mg/100 g |
| Sodium | 210.0 mg/100 g |
| Iron | 80.0 mg/100 g |
| Zinc | 100.0 mg/100 g |

The mineral content in the kernel (Table 2) reflects on the physical as well as thermal properties of composites. The tamarind seed contains polysaccharide between 60 & 65 % and is a galactoxyloglucan which is a combination of galactose, xylose, and glucan forms a highly viscous gel when in contact with hot water for around 5 minutes. TSG is biocompatible, biodegradable, non-toxic, thermally stable, and bonds hard with the reinforcement.

Tamarind kernel powder is a highly branched carbohydrate polymer chemically possesses nonnewtonian flow properties, as they are in most other hydrocolloids. The suitability of tamarind kernel powder as a carrier to boost the solubility rate of the poorly water-soluble medication celecoxib. To find a compatible reinforcement with TSG, an extensive literature review is carried out, considering the environmental aspects, three bio-degradable materials were chosen as reinforcements with TSG, namely Eggshell, Ground Nut Pod and Paper Cellulose.

Each of these reinforcements was chosen based on compatibility, manufacturability, availability, process ability, and degradability. Synthesis of samples is done to compare these reinforcements in aspects like thermal conductivity, diffusivity, and resistivity, to know which material possesses required thermal properties. Conducted morphological characterization to see the interaction of TSG with selected reinforcements.

2 Materials and Processing

The tamarind seeds are processed to get the kernel powder which is the source of gum. Tamarind seeds are available abundantly in the various parts of rural India and can be gathered from the places where the seeds are disposed off as a waste product in a larger quantity from many tamarind pulp-based farms and industries. Extraction of tamarind seed polysaccharide (gum) comprises following steps⁽⁷⁾, which involves roasting the seeds at a temperature of 110°C for 10 minutes in a pan ensuring uniform roast of testa (outer shell). The purpose of roasting is for ease of testa removal from the tamarind seed, the roasting time also varies depending on the age of tamarind seeds. After adequate roasting, the seeds are hammered to separate testa from the kernel which employs manual hammering or use of rotary hammer mill operated at low RPM. Further grinding of the seeds, done to convert the kernel into a fine powder.

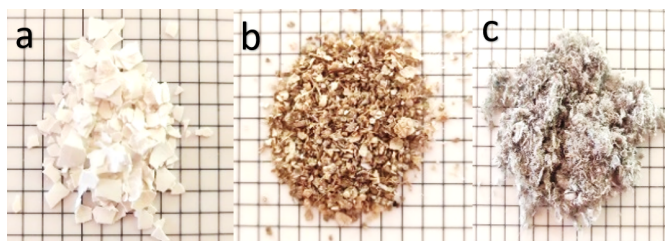


Fig 1. Processed reinforcements of eggshell (a), groundnut shell (b) and paper cellulose (c).

The gum from kernel powder is prepared by indirect heating the powder in the presence of a gum formation medium like distilled water maintained at the temperature of 100°C for approximately 15 minutes. The quantity of distilled water to be added is approximately double the mass of kernel powder utilized. The rate of evaporation of distilled water while the heating process is found out to be 3 gm/min. The gum becomes more viscous as more water gets evaporated from the mixture, which is not desirable because of the in-homogenous distribution of reinforcement in the sample.

The first reinforcement used in combination with TSG is Eggshell (Figure 1a) particulates containing calcium carbonate (CaCO₃) at large, with traces of other elements like Iron, Zinc, and Phosphorous. The ES is chosen based on its ability to sustain higher temperatures without altering the properties. The particulates are obtained by breaking the shell into a smaller size, followed by mechanical sieving to segregate uniform-sized particulates. The membrane present on the ES triggered the decaying of the sample generating a bad odour while curing. To separate the membrane from ES, the particulates are processed by treating with a moderate acid solution, followed by alkaline treatment with 5% v/v⁽⁸⁾.

The second reinforcement GP (Figure 1b) is selected based on its lower thermal conductivity⁽⁹⁾. Groundnut is one of the commercial and widely grown crops in India and is the third-largest producer of this crop⁽¹⁰⁾, is the waste product produced after extraction of nuts from its pod. Newer innovations in composite materials have emphasized the use of GP for some applications like compressed particulate boards. The GP consists of 65.7% Cellulose, 21.2% Carbohydrates, 7.3% Proteins, 4.5% Minerals and 1.2% Lipids⁽¹¹⁾. Compared to ES the processing of GP is not tedious. Mechanical grinding is employed to break the shell into fibers and these fibers can be directly employed in the synthesis of composites.

The third reinforcement PC (Figure 1c) is currently used in building insulation in the form of loose-fill insulation⁽¹²⁾, which has a lower 'k' value compared to the other two reinforcements⁽¹³⁾. The PC is processed in various stages⁽¹⁴⁾. Paper is cut into approximate sizes, followed by soaking in distilled water for 2 hours containing a small percentage of detergent powder, this helps in releasing the ink into the solution. The wet paper pieces are ground to be disintegrated into fibers, these fibers are again soaked into the distilled water for one hour to remove any residues or impurities, followed by oven drying for one hour. During this process agglomeration of some of the fibers takes place forming lumps of fiber. These lumps are separated from the rest of the fibers, soaked, ground, and dried to separate the fibers.

3 Syntheses of samples

Samples for 'k' are prepared as per the dimensions shown in Figure 3 to test in Lee's and Charlton's apparatus. Samples are synthesized by varying the composition of matrix and reinforcement and before testing, the samples are maintained at a temperature of 24°C ± 4°C for 24 Hours. A mould of dimensions 30 mm thick and 120 mm diameter is employed to prepare thermal conductivity samples considering the shrinkage and machining allowance. The combination of open and compression moulding processes is employed to synthesis the samples.

4 Characterization of sample

4.1 Morphological characterization

Characterization based on surface morphology is carried out to visualize the intensity of bonding between the matrix and the reinforcement. Figure 2 depicts the micrograph of ES and GP reinforced TSG composites of 50:50 composition. Roughness persists on the surface of the ES samples, cavities can be visualized at 200X magnification, which reduces the strength as well as 'k', as density and 'k' are correlated. Moderate interaction is seen at the interface of matrix and ES reinforcement.

Better interaction is observed between the interface of GP and TSG which enhances the strength of the composite. The specimens have less mass compared to ES based composites mainly because of the pores structure of GP also reduces the density of composites.

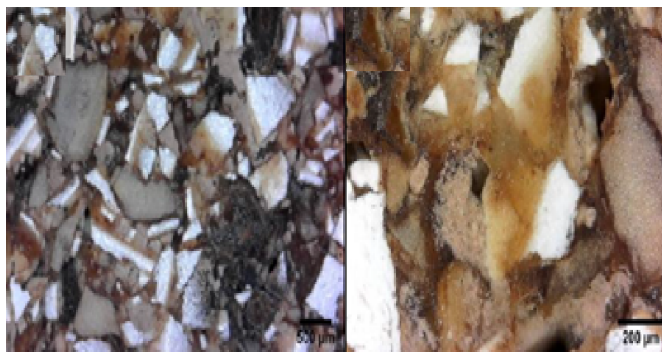


Fig 2. Optical Microscope micrograph of ES, TSG composite at 50X (Left) and 200X (Right) magnification.

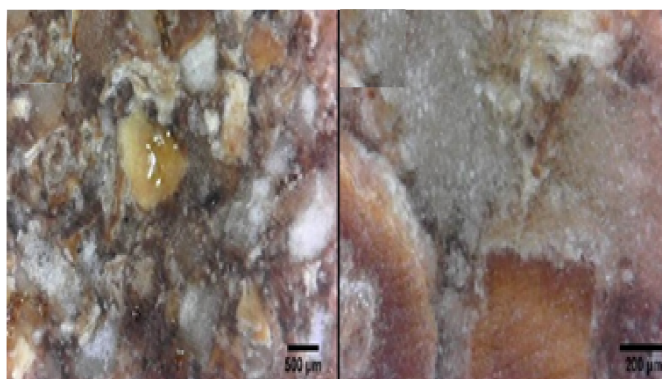


Fig 3. Optical Microscope micrograph of GP reinforced TSG composite at 50X (Left) and 200X (Right) magnification of 50:50 compositions respectively.

Morphological characterization of PCTSG composites is employed to visualize the surface characteristics of the samples. The sample with composition 30:70 (Figure 4a) has marginal interface between TSG and PC, the loose fibers are visible as adequate matrix is not present between the interface. Higher cavitation is observed in this concentration which helps to attain a lower k with reduced mass. This composition (30:70) is less prone to degradation due to minimal fungal development and retains roughness after machining. A similar phenomenon is observed in the second sample (Figure 4b) bearing the composition of 40:60. The sample of composition 50:50 (Figure 4c) shows a moderately better interface between PC and TSG with reduced cavitation which helps in attaining better strength of the composite. The sample in Figure 4d shows a better interface between TSG and PC. Tamarind seed particles of a higher size that have partially formed in the form of gum are clearly visible in the image. A higher concentration of TSG here has resulted in the reduction of cavities. The specimen with the highest concentration of TSG is seen in Figure 6e. This high concentration results in the creation of a void in the sample while curing, resulting in cavities in the sample, increasing the roughness of the machined sample.

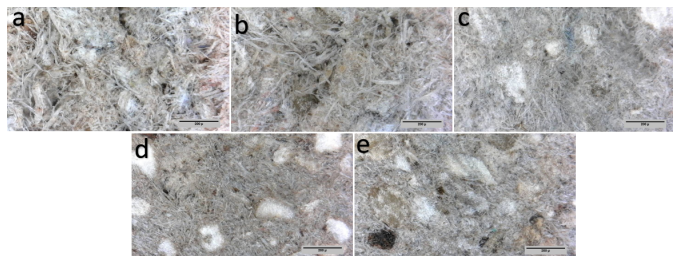


Fig 4. PCTSG composite micrographs (a,b,c,d,e) of various compositions at 50X magnification.

4.2 Fiber aspect ratio (AR)

The Aspect Ratio of the fibers significantly affects the properties of composites. Short fibers tend to increase compressive strength and long fibers tend to increase the flexural as well as tensile strength⁽¹⁵⁾. The average diameter/thickness of the cellulose fiber is found by measuring the diameters of selected samples at various places at 200X magnification by image analyzer software as depicted in Figure 5. The average of the diameters is found out to be 40.3μ.

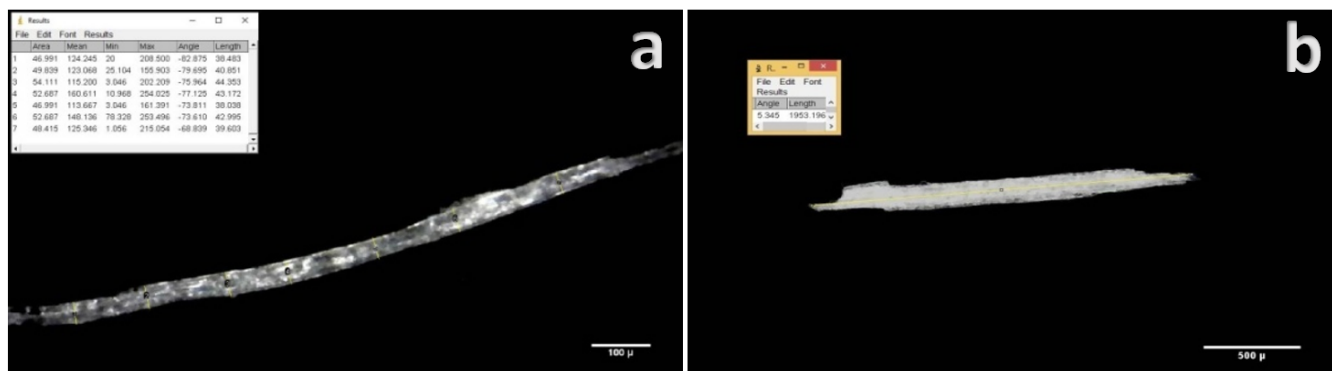


Fig 5. Microscopic image of paper cellulose fiber at 200X (a) and 50X (b) magnification.

The average length of PC fibers is calculated by considering the lengths of sample fibers at 50X magnification. The average length (L) of PC fibers is determined as 1588μ, governed by the equation of aspect ratio. The aspect ratio of PC fibers is found out to be 39.4.

$$AR = \frac{L}{d} \tag{1}$$

5 Results and discussions

Various thermal properties are tabulated which are essential to quantify the synthesized samples as thermal insulators. Based on the time-temperature data, the curve is plotted as seen in Figure 6. The linear fit is plotted on the curve to tabulate the slope of the curve. It is observed that the less steep the curve, less will be the value of slope which affects the value of k. Following equation is used to tabulate the thermal conductivity of samples; where ‘m’ is mass of brass disk, ‘s’ specific heat of disc, ‘dT/dt’ is the slope generated from the temperature variation, ‘A’ is the area of specimen, T1 and T2 are temperatures of brass disk and steam chamber respectively.

$$k = \frac{m \cdot s \cdot x \cdot \left(\frac{dT}{dt}\right)}{A(T_1 - T_2)} \tag{2}$$

Thermal conductivity values are tabulated and compared as seen in Figure 7 The thermal behaviour of ES based composites is noticed as the ‘k’ value of the sample reduces with the decrease in filler content, since the ES possess a ‘k’ value of 0.456 W/mk⁽¹⁶⁾. The higher concentration of filler content in the GP based composites possess a lower ‘k’ value and goes on increasing with the

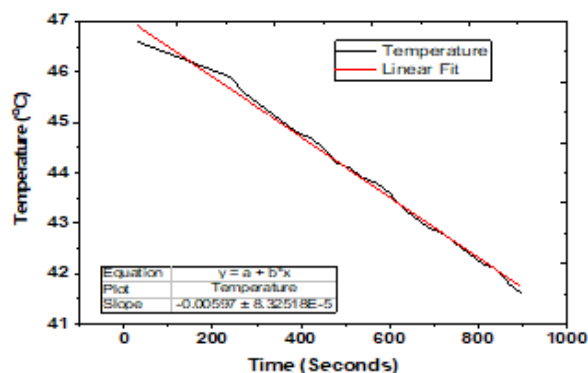


Fig 6. Slope with the linear fit (Time – Temperature Curve) of PCTSG samples.

increase in matrix content since the ‘k’ value possessed by GP is 0.12 W/mk⁽¹⁷⁾. A similar phenomenon is observed in the case of ‘PC’ based composites where cellulose possesses the ‘k’ value of 0.04 W/mk⁽¹⁸⁾. The average ‘k’ value possessed by PC based composites is 0.052 W/mk compared to other investigators possessing ‘k’ value in the range of 0.03 to 0.16 W/mk^(19,20).

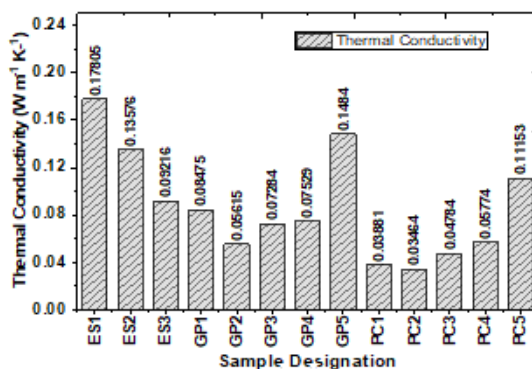


Fig 7. Thermal conductivity of eggshell (ES), groundnut shell (GP) & paper cellulose (PC) based samples.

A high-density material, by and large, maximizes weight and also is an aspect of ‘low’ thermal diffusivity and ‘high’ thermal mass, is an important property, mainly because it influences the mass and thermal conductivity of the material. The density of the samples is found out as depicted in Figure 8. ES inherently possesses higher mass; this is reflected in the samples as well. The ES based samples show the density in the range of 1.3 to 1.4 gm/cm³ which is higher in comparison. The GP based samples possess density falling in the range of 0.5 to 1.03 gm/cm³ which is better when compared with ES based composites. The PC based samples possess density in the range of 0.4 to 0.6 gm/cm³ for the filler content varying from 30% to 70%, which is better when compared with ES and GP composites.

Thermal resistance is one of the thermal properties considered for thermal insulation, can be considered as the ratio of the temperature difference between the two faces of a material to the rate of heat flow per unit area, whereas the material resists a heat flow. Thermal resistance governs the heat insulation property of a material. Lower heat loss persists for higher thermal resistance. The thermal resistance, ‘R’, is governed by two parameters which are thermal conductivity k, and the material thickness ‘h’.

$$R = \frac{h}{k} \tag{3}$$

The equation 3 is considered to calculate the thermal resistance, where instead of considering the thickness of the sample, a specific thickness is considered (100 mm) to maintain uniformity of calculation, since the composite thickness has a higher

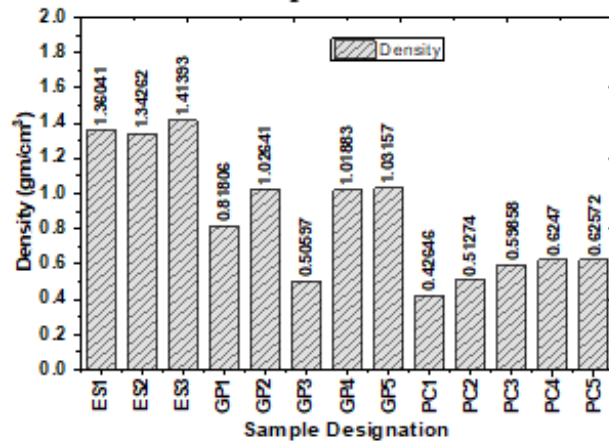


Fig 8. Density of eggshell (ES), groundnut shell (GP) & paper cellulose (PC) based samples.

influence on ‘R’ value.

The graph, as seen in Figure 9 shows the tabulated readings of thermal resistance, which shows the variation in ‘R’ value by considering the thermal conductivity of the synthesized samples. It is noted that the ‘R’ value goes on reducing with an increase in ‘k’ value, which happens because of an increase in matrix and reduction in filler content in the composite samples.

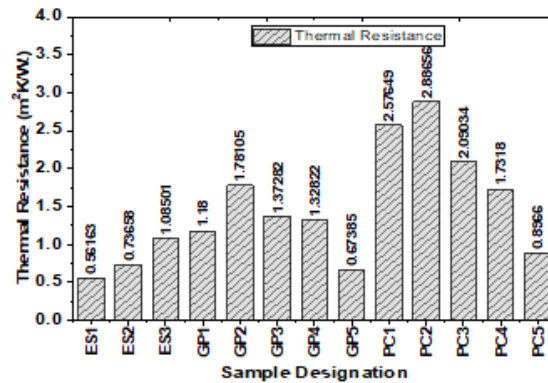


Fig 9. Thermal resistance of eggshell (ES), groundnut shell (GP) & paper cellulose (PC) based samples.

Another thermal insulation property that is thermal diffusivity (α), usually describes the rate of temperature spreading through the material. ‘ α ’ is calculated considering the thermal conductivity and the specific heat capacity of a material in terms of mm^2/s . Thermal diffusivity is a material-specific property, varies with the composition of the material in composites and characterized by unsteady conduction of heat. The ‘ α ’ value describes how rapidly a composite responds to change in the temperature. Figure 10 shows the variation in ‘ α ’ values of respective samples, where the average α value of the ES, GP, and PC samples is 1.22, 0.946, and 0.829 $\text{m}^2\text{W}/\text{K}$ respectively. The α value fairly decreases with an increase in TSG and decreases with an increase in filler content. As thermal insulation is considered, the α should be lower in order to resist the diffusion of heat through the composite. The ‘ α ’ is determined by the following equation; where ‘ ρ ’ is density of sample.

$$\alpha = \frac{k}{\rho \times C_p} \tag{4}$$

The Specific Heat Capacity (c_p) of material is basically the amount of heat necessary to raise the temperature of 1kg of the material by 1K or by 1°C. A good insulator should have a ‘ c_p ’ value which makes it take up more time to absorb the heat before it really heats up to transfer the heat content. Higher ‘ c_p ’ is the feature of materials to provide thermal mass or thermal buffering for

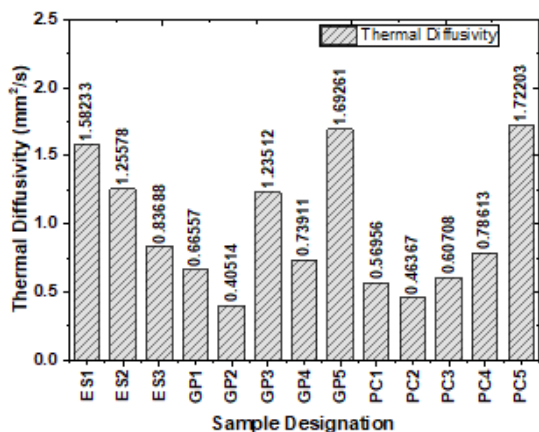


Fig 10. Thermal diffusivity of eggshell (ES), groundnut shell (GP) & paper cellulose (PC) based samples.

heat transfer. Figure 11 shows the ‘ c_p ’ of samples, where results of ‘ c_p ’ of samples are tabulated by Rule of Mixtures, considering the c_p values of fillers and Tamarind seed powder. Higher ‘ c_p ’ values are seen in the lower composition of TSG and higher filler content in the case of GP and PC composites, whereas ES based composites show marginal variation in the ‘ c_p ’.

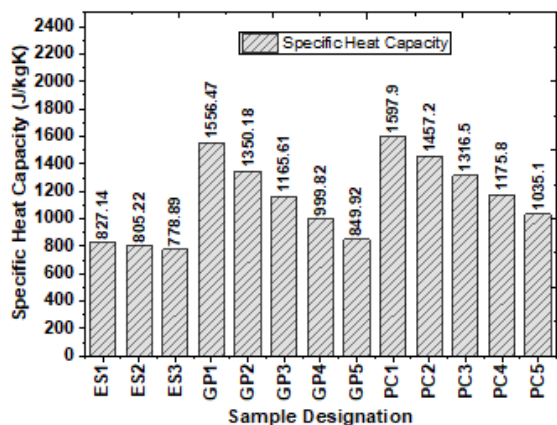


Fig 11. Specific Heat Capacity of eggshell (ES), groundnut shell (GP) & paper cellulose (PC) based samples.

6 Correlation between density and thermal conductivity

To conduct heat effectively a physical medium is essential, increase in density basically means a material has more mass to conduct heat, whereas the composites with lower density contain small air pockets, which makes it to possess lower thermal conductivity since the air possesses ‘ k ’ value around 0.02W/mk. Figure 12 shows the scatter diagram of the ES, GP, and PC samples. It can be seen that the lower density samples possess lower ‘ k ’ value and as the density of samples varies, the corresponding variation in ‘ k ’ value is noticed.

7 Theoretical model for thermal conductivity

Many theoretical models have been derived based on the two-phase mixtures⁽²¹⁾ to predict the effective thermal conductivity of the materials based on the factors like direction of heat flow, the arrangement of materials, and the size of filler material. All

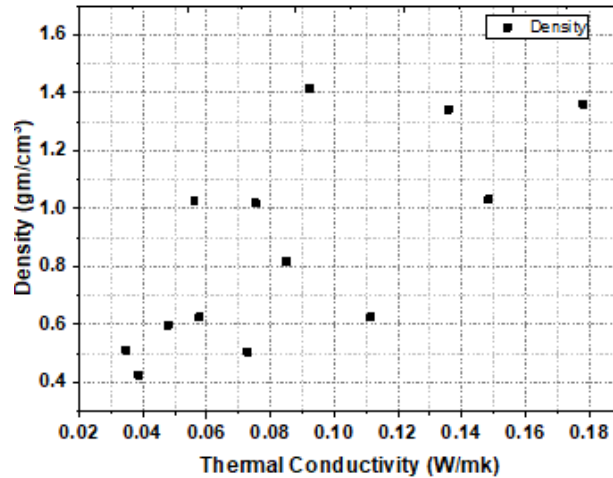


Fig 12. Scatter diagram for density vs thermal conductivity of eggshell (ES), groundnut shell (GP) & paper cellulose (PC) based samples.

the theoretical models are derived on three inputs, which are thermal conductivity of matrix (k_m), the thermal conductivity of filler (k_f), and the volume fraction of filler (φ). One of the commonly used models is Series Model which can be seen in the below equation:

$$\frac{1}{k_c} = \frac{1 - \varphi}{k_m} + \frac{\varphi}{k_f} \tag{5}$$

For Parallel Model the equation derived is:

$$k_c = \varphi \cdot k_f + (1 - \varphi) \cdot k_m \tag{6}$$

Maxwell’s equation is considered for lower concentrations of filler material in which the filler is in contact with the matrix but not with filler. The Maxwell model is derived as:

$$k_c = k_m \left[\frac{k_f + 2 \cdot k_m + 2 \cdot \varphi (k_f - k_m)}{k_f + 2 \cdot k_m - \varphi (k_f - k_m)} \right] \tag{7}$$

Russel developed the model assuming the discrete phase are isolated cubes dispersed in the matrix, this model is a combination of series and the parallel network is as shown below:

$$k_c = k_m \left[\frac{\varphi^{\frac{2}{3}} + \frac{k_m}{k_f} (1 - \varphi^{\frac{2}{3}})}{\varphi^{\frac{2}{3}} - \varphi + \frac{k_m}{k_f} (1 + \varphi - \varphi^{\frac{2}{3}})} \right] \tag{8}$$

Figure 13 shows the comparison of the experimental results for thermal conductivity of samples with the results of various theoretical models, consistent deviation in the experimental and theoretical results is observed except for the samples namely GP5 and PC5 possessing the highest concentration of filler content. This variation is assumed to be the material density and homogeneity of synthesized composites.

8 Conclusion

Nature is filled with a variety of materials, a combination of which we can produce in the form of composites that possess various properties. An effort is made in the present work to utilize some of the materials which are naturally available in nature and to synthesize the composites, test, and find the thermal properties. Considering complete bio-degradability and environmental

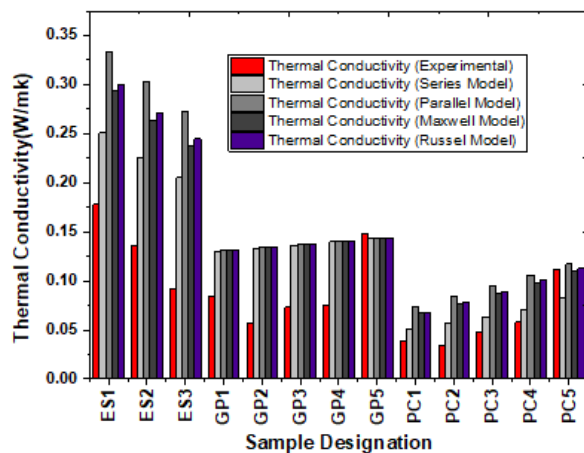


Fig 13. Experimental (ES, GP & PC) and theoretical thermal conductivity models.

aspects, based on literature, Tamarind Seed Gum is used as a matrix, and Egg Shell, Ground Nut Pod, and Paper Cellulose are considered as reinforcements, further these reinforcements are used in combination with TSG to synthesize the samples for testing. Based on the test results selection of single reinforcement is done for further investigation. It is noticed that the k , ρ , R , α , and c_p values of ES does not fall in the required range, which raises the question of its suitability as thermal insulators, however the ES's performance is better at elevated temperatures. The GP composites moderately possess the required values in comparison with ES but degrade in properties at elevated temperatures. PC composites possess the required values compared to ES and GP. The average 'k' value possessed by PC based composites is lower than ES and GP composites, making it ideal composite for insulation applications, as cellulose is employed in the form of loose fillings, this research fulfilled the need for it to be used in the form of biodegradable composites. Morphological characterization showed the compatibility between the matrix and reinforcement used which further affects the strength of the composite. In the effort of finding better properties from the composites, there is a trade-off between lower 'k' value and high-temperature performance.

References

- 1) Al-Mudhaffer AF, Saleh SK, Kadhum GI. The role of sustainable materials in reducing building temperature. *Materials Today: Proceedings*. 2021. Available from: <https://doi.org/10.1016/j.matpr.2021.08.249>.
- 2) Dickson T, Pavia S. Energy performance, environmental impact and cost of a range of insulation materials. *Renewable and Sustainable Energy Reviews*. 2021;140(110752):110752–110752. Available from: <https://doi.org/10.1016/j.rser.2021.110752>.
- 3) Hamdani MMA, Bekkouche SMA, Benouaz TK, Cherier MK, Belarbi R. Interior Insulation of Walls Exposed by Polystyrene in South Algeria. *Indian Journal of Science and Technology*. 2018;11(7):1–6. doi:10.17485/ijst/2018/v11i7/120903.
- 4) Oladele TIO, Omotosho AF, Adediran A. Polymer-Based Composites: An Indispensable Material for Present and Future Applications. *International Journal of Polymer Science*;2020. Available from: <https://doi.org/10.1155/2020/8834518>.
- 5) Kushal G, Ambli, Bhimanagoud M, Dodamani JA, Vanarotti MB. Heterogeneous composites for low and medium temperature thermal insulation: A review. *Energy & Buildings*. 2019;199:455–460. Available from: <https://doi.org/10.1016/j.enbuild.2019.07.024>.
- 6) Anjali G, Sharma V, Jain S. Nutritional Properties of Tamarind (*Tamarindus Indica*) Kernel Flour. *International Journal of Current Microbiology and Applied Sciences*. 2020;9(5):1359–1364. Available from: <https://doi.org/10.20546/ijcmas.2020.905.153>.
- 7) Yadav A, Vishwakarma RK, Mishra SK, Shukla AK. Isolation and Characterization of Tamarind Seed Gum as Pharmaceutical Excipient. *International Journal of Health and Clinical Research Res*;2020:49–57.
- 8) Pazarin D, Rovinaru C. Separation Methods of the Eggshell Membranes from Eggshell. *Priorities of Chemistry for a Sustainable Development-PRIOCHEM*. 2019;29:122–122. Available from: <https://doi.org/10.3390/proceedings2019029122>.
- 9) Duc PPA, Dharanipriya B, Velmurugan MK, Shanmugavadivu. Groundnut shell -a beneficial bio-waste. *Biocatalysis and Agricultural Biotechnology*. 2019;20:101206–101206. Available from: <https://doi.org/10.1016/j.bcab.2019.101206>.
- 10) Musekiwa P, Moyo LB, Mamvura TA, Danha G, Simate GS, Hlabangana N. Optimization of pulp production from groundnut shells using chemical pulping at low temperatures. *Heliyon*. 2020;6(6):e04184–e04184. Available from: <https://doi.org/10.1016/j.heliyon.2020.e04184>.
- 11) Alaneme KK, Bodunrin MO, Adebimpe A. Awe, Microstructure, mechanical and fracture properties of groundnut shell ash and silicon carbide dispersion strengthened aluminium matrix composites. *Journal of King Saud University - Engineering Sciences*. 2018;30(1):96–103. Available from: <https://doi.org/10.1016/j.jksues.2016.01.001>.
- 12) Kwon YC, Yarbrough DW. Cellulose Insulation for Use as Building Insulation in Korea. *International Conference on Advanced Materials Science and Civil Engineering*. 2017;70. doi:10.2991/amsce-17.2017.18.
- 13) Gupta P, Singh B, Agrawal AK, Maji PK. Low density and high strength nanofibrillated cellulose aerogel for thermal insulation application. *Materials & Design*. 2018;158:224–236. Available from: <https://doi.org/10.1016/j.matdes.2018.08.031>.

- 14) Aquino FDCR, Carlos F, Padua H, Tayactac. Adrienne Hera Zulueta, Erison Roque, and Nuna Almanzor. *MATEC Web of Conferences*. 2019;268:4013–4013. Available from: <https://doi.org/10.1051/mateconf/201926804013>.
- 15) Yoo DY, Kim S, Park GJ, Park JJ, Kim SW. Effects of fiber shape, aspect ratio, and volume fraction on flexural behavior of ultra-high-performance fiber-reinforced cement composites. *Composite Structures*. 2017;174:375–388. Available from: <https://doi.org/10.1016/j.compstruct.2017.04.069>.
- 16) C165-07(2017) A. Standard Test Method for Measuring Compressive Properties of Thermal Insulations, ASTM International, West Conshohocken, PA. ASTM International. 2017. Available from: www.astm.org.
- 17) Venkata SP, Bitra S, Banu P, Ramakrishna G, Narender AR, Womac. Moisture dependent thermal properties of peanut pods, kernels, and shells. *bio systems engineering*. 2010;106:0–3. doi:10.1016/j.biosystemseng.2010.05.016.
- 18) Uetani K, Hatori K. Thermal conductivity analysis and applications of nanocellulose materials. *Science and Technology of Advanced Materials*. 2017;18(1):877–892. doi:10.1080/14686996.2017.1390692.
- 19) Ninikas K, Mitani A, Koutsianitis D, Ntalos G, Taghiyari HR, Papadopoulos AN. Thermal and Mechanical Properties of Green Insulation Composites Made from Cannabis and Bark Residues. *Journal of Composites Science*;5(5):132–132. Available from: <https://doi.org/10.3390/jcs5050132>.
- 20) Liu ZTW, Wang GZ, Li G, Shi X, Zhao. Mechanical properties and thermal conductivity of lightweight thermal insulation composites. *The 7th Global Conference on Materials Science and Engineering*. 2019;474:12038–12038. doi:10.1088/1757-899X/474/1/012038.
- 21) Mohapatra RC, Mishra A, Bhushan B, Choudhury. Experimental Study on Thermal Conductivity of Teak Wood Dust Reinforced Epoxy Composite Using Lee's Apparatus Method. *International Journal of Mechanical Engineering and Applications*. 2014;2(6):98–98. doi:10.11648/j.ijmea.20140206.13.